Materials Advances

ROYAL SOCIETY OF CHEMISTRY

PAPER

View Article Online
View Journal | View Issue

Cite this: *Mater. Adv.*, 2024, 5, 2088

Antibiotic-loaded gelatin fibers fighting bacteria resistant to antibiotics: a case of spectinomycin-resistant *Escherichia coli*†

Laura Larue,[a] Laurent Michely,[a] Xenia Moreno,[a] Rémy Pires,[a] André Pawlak,[bc] Daniel Grande[a] and Sabrina Belbekhouche*[a]

Infection with antibiotic-resistant bacteria can lead to higher mortality, morbidity, and healthcare costs. An open wound is highly susceptible to microbial infection. To encourage prompt healing, a wound requires a biomimetic dressing material, ideally with hydrophilic and antimicrobial properties. Herein, we propose hydrophobic, cargo-loaded gelatin fibers useable against antibiotic-resistant bacteria. Scanning electron microscopy (SEM) demonstrated the successful formation of the hydrophilic fibers and allowed us to characterize the morphology and the average fiber diameter before and after hydrophobic cargo loading. Differential scanning calorimetry (DSC) measurements indicated that the gelatin-based fibers may have undergone renaturation after electrospinning. Dynamic mechanical analysis (DMA) measurements showed that the presence of hydrophobic cargo enhanced the mechanical properties of the gelatin fibers without the necessity of a crosslinking step. The measurements were then repeated for the fiber when loaded with ciprofloxacin, a hydrophobic antibiotic. The *in vitro* antibacterial property of the designed ciprofloxacin-loaded gelatin fibers was evaluated by film-diffusion against spectinomycin-resistant *Escherichia coli*. An inhibitory effect on bacterial growth in a solid medium was observed. These findings demonstrated the potential of the designed fiber to be used as an antimicrobial material for the prevention and treatment of wound infections, particularly those resistant to antibiotic therapy.

Received 18th December 2023,
Accepted 11th January 2024

DOI: 10.1039/d3ma01140b

rsc.li/materials-advances

1. Introduction

Antimicrobial resistance (AMR) is a growing global threat.[1] More than 2.8 million antibiotic-resistant infections are acquired each year in the USA, resulting in an annual mortality of 35 000.[2] The O'Neill report stated that annual deaths caused by AMR could rise from above 700 000 to nearly 10 million by 2050 worldwide.[3] Antimicrobial therapy may result in wound infections in settings where infection prevention and control measurements are inadequate.[4] The burden of antibiotic-resistant infections in various types of wounds has increased.[5] The predominant bacterial isolates from infected wounds include *Escherichia coli*, *Staphylococcus aureus*, *Klebsiella pneumoniae*, *Pseudomonas aeruginosa*, *Proteus* species, and *Acinetobacter baumannii*.[6,7] Over the last decade, there has been a drive to develop new antibiotic analogs and identify new antibacterial therapies.[8]

In addition to antibiotic resistance, healing of full thickness wounds is also an issue, as wounded skin does not spontaneously regenerate. Prompt closure of the wound requires a skin regeneration product. Consequently, a tissue engineered scaffold enriched with an antimicrobial compound would be of major interest for application to full thickness wounds. Electrospinning is one of the most widely used techniques used to produce polymeric nanofibers[9] and eventually to construct a tissue engineered scaffold as a carrier for the delivery of antibiotics. Electrospun nanofibers have various attractive properties which make them suitable candidates for wound dressings. These include (i) a large surface area-to-volume ratio and a highly porous structure, which attracts fibroblasts for extracellular matrix component secretion and the activation of cell signaling,[10] (ii) allowing drug loading to behave as drug delivery materials[11] with a controlled release profile, and (iii) highly interconnected pores which protect the wound from microbial infiltration.[12,13] Numerous polymers, ranging from synthetic macromolecules, such as poly(ε-caprolactone), poly(lactic-*co*-glycolic acid), poly(ethylene oxide), and poly(lactic acid), to natural polymers such as collagen, chitosan, silk, fibroin, hyaluronic acid, and gelatin, have been utilized to fabricate

[a] *Univ Paris Est Creteil, CNRS, Institut de Chimie et des Matériaux Paris-Est (ICMPE), UMR 7182, 2 Rue Henri Dunant, 94320 Thiais, France. E-mail: sabrina.belbekhouche@cnrs.fr; Tel: +33 1 49 78 11 49*
[b] *Institut National de la Santé et de la Recherche Médicale (INSERM), IMRB U955, Créteil, F-94010, France*
[c] *Univ Paris Est Creteil, Faculté de Médecine, UMRS 955, Créteil, F-94010, France*

† Electronic supplementary information (ESI) available. See DOI: https://doi.org/10.1039/d3ma01140b

nanofibers for specific drug-delivery and tissue regeneration applications.[14] Gelatin is a biopolymer obtained from the partial hydrolysis of collagen, the principal extracellular matrix building protein. Since it can be extracted from the hydrolysis of skin or tendons, gelatin is abundant, cheap, and has been approved as a non-toxic material by the Food and Drug Administration (FDA).[15]

Gelatin is a polyelectrolyte in an aqueous solution, making electrospinning gelatin challenging due to the repulsive forces among the polycations. Conditions have been found for fabricating gelatin-containing nanofibrous composites using electrospinning.[16–19] Gelatin solutions with concentrations ranging from 5 to 12.5% weight per volume (w/v) in 2,2,2-trifluoroethanol (TFE) have been electrospuned into fibers with an average diameter ranging from 100 to 340 nm.[18] Using 98% formic acid as a solute, gelatin solutions with concentrations between 7 and 12% wt/v have been electrospuned into nanofibers with an average diameter ranging from 70 to 170 nm.[19]

Ciprofloxacin(1-cyclopropyl-6-fluoro-1,4-dihydro-4-oxo-7-(1-piperazinyl)-3-quinoline carboxylic acid) is a fluoroquinolone antibiotic commonly used to treat various bacterial infections, including those involving the skin or soft tissues.[20] Due to its low minimal inhibitory concentration and the low prevalence of microbial resistance, ciprofloxacin is often used to treat wound infections.[21] However, its potential benefits are limited by its poor water solubility (solubility less than or equal to 1 mg mL^{-1} in water), short half-life, and low bioavailability. These shortcomings may be overcome by administering the drug through an alternative approach.

There have been reports on the incorporation of ciprofloxacin into synthetic polymeric fibers and the evaluation of their antibacterial activity.[21–23] For instance, Kataria *et al.* fabricated electrospun nanofibers loaded with ciprofloxacin hydrochloride in microporous materials composed of poly(L-lactide-*co*-D,L-lactide) and poly(ethylene glycol). Microbiological tests with *Staphylococcus aureus* were performed on such material and revealed that the fiber mats inhibited bacterial growth.[24] Few reports have described the loading of this antibiotic in natural polymers, such as dextran or chitosan.[25] For example, Unnithan *et al.* developed dextran/polyurethane fibers loaded with ciprofloxacin hydrochloride and found that they had good bactericidal activity against both Gram-positive and Gram-negative bacteria.[21] Alginate/poly(ethylene oxide) composite fibers were also fabricated and reported for loading with ciprofloxacin hydrochloride but without examining the antibacterial properties.[26] In the cited approach and in most of the work reported on the loading with ciprofloxacin hydrochloride, *i.e.* under the hydrochloride salt form of ciprofloxacin. Thus, very few studies trap this antibiotic in its non-protonated form, *i.e.* ciprofloxacin. For example, Aytac *et al.* exploited cyclodextrin chemistry to load ciprofloxacin in two steps. They fabricated in water media gelatin nanofibers encapsulating ciprofloxacin through complexation with cyclodextrin in two steps. Step 1 consists in entrapping the ciprofloxacin in cyclodextrin and step 2 consists in loading the as-obtained complex in gelatin solubilized in acetic acid media but they did not perform any bacterial assay or any biological test.

Although many researchers have fabricated ciprofloxacin (protonated or not) -loaded nanofibers for antibacterial purposes, to the best of our knowledge, electrospun nanofibers have not hitherto been loaded with ciprofloxacin for use against antibiotic-resistant bacteria. Therefore, in the present investigation, gelatin-based nanofibers loaded with ciprofloxacin have been prepared for this purpose. We therefore propose to trap ciprofloxacin in its non-protonated form in gelatin in a single step in an organic solvent (trifluoroethanol) that is totally removed at the end of the process. Note that gelatin is electrospinnable only from solutions in which this macromolecule has a random coil conformation. In aqueous solutions below 30 °C, the gelation occurs resulting in the impossibility of electrospin at room temperature. Furthermore, the high surface tension of aqueous solutions complicates electrospinning because of the destabilization of polymer jets and the droplet formation. Water has a high boiling temperature which leads to an additional problem, *i.e.* non-complete water evaporation before reaching the collector. This results in fibers fusion and heterogeneities. For instance, Lu *et al.* utilized water as a solvent to electrospin pure gelatin solution. They found that at low concentrations of gelatin, the viscosity was insufficient to generate continuous nanofibers, resulting in the formation of unwanted microbeads. However, at a high concentration of gelatin (>25%), the spinning solution became too viscous, which seriously inhibited efficient electros pinning, leading to few nanofibers.[27]

Herein, we aim to design electrospun mats for the purpose of antibacterial drug delivery. We have used gelatin as a biological polymer to favor biocompatibility. We have produced hydrophobic cargo-loaded gelatin fibers to assess the mechanism of cargo release. We first used Nile red as a probe for the proof of concept, and then the hydrophobic antibiotic ciprofloxacin. These two compounds have similar solubility in aqueous media, which is less than 1 g L^{-1}. Using the electrospinning technique, we have produced fibers loaded with the above-mentioned cargoes from a solution of gelatin in trifluoroethanol and demonstrated the subsequent effective removal of trifluoroethanol after fiber formation. We have then characterized the morphological, structural, and thermal properties of the nanofibers by several physico-chemical techniques, including SEM, FTIR, DSC and DMA. From DSC measurements, we infer that the gelatin-based fiber may have undergone renaturation after electrospinning. Using DMA measurement, we were able to show that the presence of hydrophobic cargo enhances the mechanical properties of the gelatin fiber. This result is of interest as previous literature has shown that there is an enhancement of the mechanical properties of gelatin fibers after film crosslinking.[28] We have also characterized the kinetics of hydrophobic release from gelatin hybrid fibers in physiological fluid (phosphate-buffered saline, pH = 7.4) before going on to characterize the release of the hydrophobic antibiotic ciprofloxacin from the gelatin fibers. Lastly, we have measured the effect of the loaded gelatin fiber on the growth of antibiotic-resistant bacteria in culture, namely spectinomycin–resistant *Escherichia coli* (*E. coli*). Two types of tests have been performed with the ciprofloxacin-loaded fibers, *i.e.* (i) a direct biofilm contact assay and (ii) an inhibitory growth assay. Spectinomycin is a broad-spectrum antibiotic that belongs to the aminocyclitol class. This antibiotic

is included in the World Health Organization (WHO) model list of essential medicines.

2. Experimental section

2.1. Materials

Gelatin type A from porcine skin (gel strength 300 g Bloom), Nile red, phosphate-buffered saline (PBS); trifluoroethanol (TFE) and ciprofloxacin were purchased from Sigma-Aldrich. Lysogeny broth (LB) Miller culture medium was purchased from Fischer Scientific. The chemicals were used without further purification. Water at 18 MΩ was produced by MilliQ (Millipore).

2.2. Preparation of the spinning solutions and electrospinning of gelatin/Nile red and gelatin/ciprofloxacin nanofibers

To prepare the spinning solutions, the gelatin was dissolved in TFE at 7.5% weight per volume (w/v) by gentle stirring at room temperature for 12 h, after which a transparent solution was obtained. 7.5% w/v means that 0.75 g of gelatin powder was mixed with 10 mL of TFE solvent. The hydrophobic cargo (Nile red or ciprofloxacin) was loaded by mixing it with the 7.5% w/v gelatin/TFE solution under stirring conditions for 12 h.

The gelatin-based solution was loaded in a syringe. A syringe pump was used to feed the solution through a needle. The flow rate of the solution was fixed to 0.8 mL h^{-1} and a 25 kV potential difference was applied between a metal capillary (injector at 15 kV) and a metal plate (flat collector at −10 kV). A piece of aluminum was deposited on the plane collector to collect the fibers. The electrospinning was carried out at room temperature under atmospheric air and the fibers were collected for 4 h and were dried under vacuum for 24 h.

2.3. Preparation of gelatin film

We dissolved 375 mg of gelatin in 5 mL of TFE(7.5% w/v concentration), over 24 h at room temperature. The gelatin solution was then poured into a glass Petri dish and placed on a hot plate at 40 °C overnight in a fume hood to evaporate the whole solvent and was dried under vacuum for 24 h.

2.4. Physico-chemical characterization of the gelatin based material

Microscopic observations. The morphology and diameter of the electrospun fibers were examined using an optical fluorescence ZEISS microscope (LSM 700 Laser Scanning Microscope, Carl Zeiss, France) and a scanning electron microscope (SEM) (MERLIN microscope from Zeiss). Prior to SEM analysis, the samples were coated with a 4 nm layer of palladium alloy in a Cressington 208 HR sputter-coater.

Physico-chemical characterization. Fourier-transform infrared (FTIR) spectra were recorded between 4000 and 400 cm^{-1} using a Bruker Tensor 27 spectrometer (Bruker Optik GmbH, Germany). The samples were placed on the crystal of the ATR accessory and 32 co-added scans at 4 cm^{-1} resolution were taken for each sample.

Thermogravimetric analysis (TGA) was carried out using a Setaram LabSys thermobalance in air over a temperature range from 30 to 800 °C at a heating rate of 20 °C per minute.

Differential scanning calorimetry (DSC) analyses were carried out using a TA Instruments Discovery 25 series calorimeter from 10 °C to 250 °C, and heating rates of 10, 20, and 40 °C min^{-1} in sealed crucibles to determine the melting temperature of the crystalline part of gelatin (T_m); the glass transition temperature of the amorphous part of gelatin (T_g); the denaturation temperatures (T_d and $T_{d'}$); and denaturation enthalpy (ΔH_d) of gelatin-based materials. Modulated tests were also carried out.

Dynamic mechanical analysis (DMA) experiments using TA instruments were performed for mechanical tests. 3 to 5 tensile tests at a speed of 1 mm min^{-1} at 25 °C were carried out on rectangular specimens from each sample.

2.5. Bactericidal activity of gelatin material loaded with ciprofloxacin

Bacteria cultivation and plate preparation for agar diffusion tests. Nutrient LB agar plates (9 cm diameter filled with 20 ± 0.1 mL of LB agar) were inoculated separately with 1 mL of the spectinomycin-resistant *E. coli* cultures whose absorbance at 600 nm was adjusted to 0.2 by dilution in LB broth.

Agar diffusion tests. Two antibacterial assays were performed. The first one consisted of a direct biofilm contact test to assess bacterial killing in the biofilms. The second was an inhibitory growth test to investigate the ability of the gelatin-based fiber to prevent bacterial growth around the sample. In the first approach, inoculated plates were incubated overnight at 37 °C to enable the biofilm formation on the nutrient surface. A gelatin-based fiber material was then deposited on the surface and some plates were incubated for 24 h and others for 48 h before checking. In the second assay, a gelatin-based fiber material was deposited, just after the plate had been inoculated with spectinomycin-resistant *E. coli* (as previously described), and the plates (containing spectinomycin-resistant *E. coli* and gelatin-based fiber) were then incubated at 37 °C.

For both tests, the antibiotic activity of the gelatin-based fiber samples was assessed by the appearance over time of clear zones (inhibition zones) around the samples. Clear zones were defined as zones where agar was clearly visible compared to the formed biofilm that covered the agar. The clear zones corresponded to areas where bacteria were killed in the first assay, and to zones where bacterial growth had been inhibited in the second. Each test was reproduced independently at least three times. For each experiment, negative control plates were run in parallel: plates with bacteria but without material (to confirm the gelatin-based fiber action), and plates without bacteria or material (to rule out cross-contamination).

Bacterial viability assay. The effect of gelatin based fibers on bacterial viability was examined *via* an orange acridine test coupled with fluorescence microscopy observation. 10 μL of acridine orange (0.1 wt%) was added to 100 μL of bacterial suspension taken at the end of the antibacterial assay. A 10 μL drop of this mixture was then taken up and introduced on a cover slip to investigate the bacteria viability.[29]

3. Results and discussion

One of the main issues associated with currently used antimicrobial materials is their highly toxic and irritant effects on humans. Developing new strategies for the design of cost-effective and safe biocide systems is therefore of major interest.

In this context, this work aims at designing electrospun mats (ESM) for antibacterial drug delivery purposes (against antibiotic-resistant bacteria). Our motivation was to design a system only based on a biological macromolecule to favor perfect biocompatibility. We thus propose the use of gelatin, a hydrophilic biopolymer obtained from partial hydrolysis of collagen and the principal extracellular matrix building protein.[15] Toward this aim, gelatin electrospun mats were fabricated and fully characterized then a model of a hydrophobic drug namely the Nile red was loaded. Based on the results obtained from the model drug, ciprofloxacin loaded ESM was fabricated and tested against spectinomycin-*resistant E. coli* to assess the bactericidal behavior of the designed fibers.

3.1. Gelatin fibers

In water, gelatin can be easily dissolved by increasing the temperature above 40 °C, and an aqueous gelatin solution can be used to fabricate large diameter gelatin fibers by wet spinning. These fibers can have hemostatic applications.[30] However, gelatin solutions dissolved in water cannot be electrospun into ultra fine fibers even under non-gelation conditions and when heated. This is likely due to its polyelectrolyte nature. Due to this poor fiber-formation capacity of gelatin, other synthetic polymers are often added to enhance fiber formation.

Unlike synthetic macromolecules, which are generally non-ionic and can be easily dissolved in organic solvents through non-ionic interactions between solute and solvents, gelatin is a polyelectrolyte polymer with many ionizable groups. The gelatin amine and carboxyl functional groups (Fig. 1A) can be ionized by acidic agents or hydrolyzed to induce positive or negative charges. In aqueous solution, such pH-dependent ionization gives rise to a polyion bearing many charges, accompanied by many small counterions. Moreover, the strong hydrogen bonding of the gelatin results in a three-dimensional polymer network which induces that the mobility of the macromolecule chains is reduced. Although water is typically employed to prepare a gelatin solution, searching for an alternative organic solvent is crucial to successfully electrospin this biopolymer.

Gelatin has strong polarity. There are very few high-polarity organic solvents available for dissolving this macromolecule. Fluorinated alcohols, such as hexafluoroisopropanol (HFIP) and trifluoroethanol (TFE), are known to be good solvents for polypeptides, such as collagen. For instance, Matthews *et al.* successfully used HFIP as a solvent to form nanofibers from electrospun collagen fiber.[31] In this work, we used TFE to directly electrospin a gelatin solution in the presence of a hydrophobic cargo (Nile red, and the antibiotic ciprofloxacin; Fig. 1) into ultra fine fibers without adding any other synthetic material for fiber formation. The challenge is to solubilize all of these components together with TFE and, as it has a possible biomedical application, to check the TFE removal after the fiber formation. TFE was also selected because of its relatively high boiling point of around 70 °C, which offers the advantage of a lower probability of clogging the needle orifice during the electrospinning process.

The examined gelatin solutions at 7.5% w/v concentration were spinnable. Under SEM (Fig. 2A), we found that smooth nanofibers were obtained, with no bead formation. Based on these SEM pictures, the fiber diameters were analyzed using the image visualization software ImageJ. We found a diameter ranging from 100 to 300 nm (averaged diameter = 150 nm).

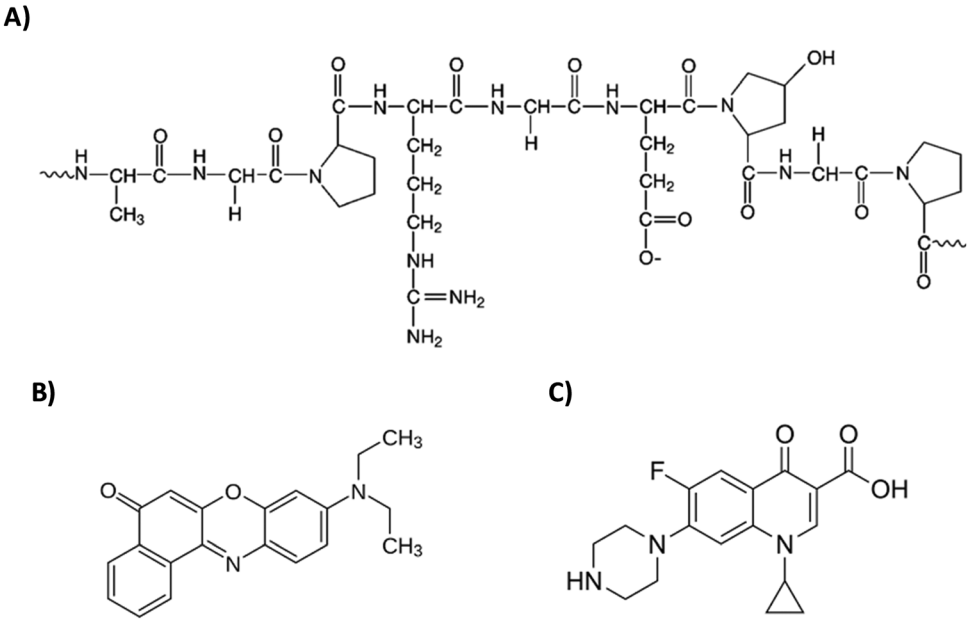

Fig. 1 Chemical structures of (A) gelatin, (B) Nile red, and (C) ciprofloxacin.

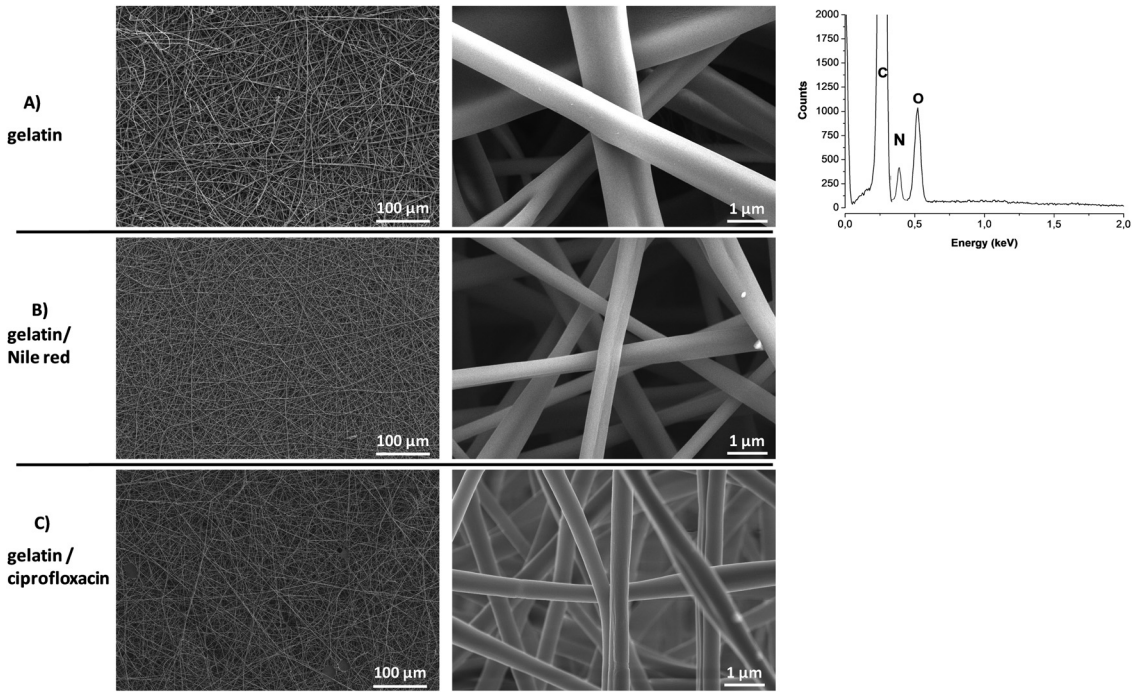

Fig. 2 SEM/EDX images of gelatin, gelatin/Nile red, and gelatin/ciprofloxacin fibers.

Our results were concordant with those of Huang *et al.*,[18] who performed electrospinning of 5% to 12.5% w/v gelatin solutions prepared in TFE. They produced fibers with an average diameter ranging from 100 to 340 nm. The presence of atomic fluor was not detected by energy dispersive X-ray (EDX) analysis (Fig. 2), corroborating the complete elimination of TFE from the fiber during the electrospinning process.

Now that we have determined the right conditions for producing gelatin-based fibers, we can move on to the next step, which involves loading these fibers with a model hydrophobic drug, namely the Nile red.

3.2. Nile red loaded inside gelatin fibers

The Nile red dye (Fig. 1B) was chosen as a model because, like ciprofloxacin (Fig. 1C), it is poorly water soluble. It could also be quickly demonstrated that this hydrophobic cargo was incorporated into the gelatin material. When Nile red was doped into the electrospun fibers with gelatin, the resulting gelatin fibers showed high fluorescence intensity (Fig. 3), thus indicating the high incorporation of Nile red into the gelatin material. Gelatin fibers alone do not show fluorescence.

Fig. 2B shows SEM images of the electrospun fluorescent fibers (gelatin/Nile red as-obtained). All electrospun fibers have straight, random fiber orientations entangled in a 3D network, and there are no beads which are formed over all extents.

The FTIR spectra of as-obtained gelatin/Nile red electrospun fibers are depicted in Fig. 4. The amide I and II characteristic bands for gelatin were observed at 1635 and 1541 cm^{-1}, respectively.[32] They corresponded to the stretching of C═O, and the combined bending of N–H and stretching of C–N, respectively.[33] The characteristic bands of gelatin could also be

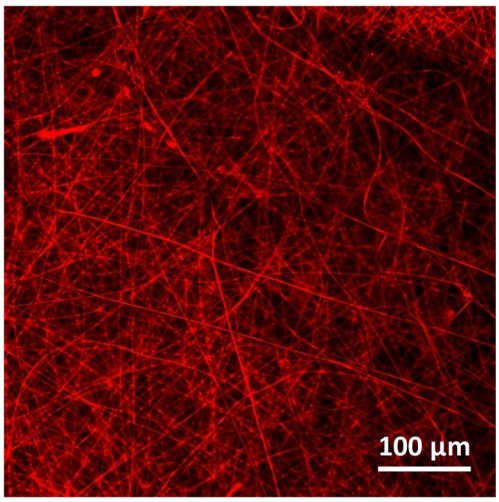

Fig. 3 Fluorescence image of Nile red/gelatin material.

detected in the gelatin/Nile red fibers at 2918 (C–H), 1635 (C═O), 1541 (C–N), 1338 (C–N), and 1078 cm^{-1} (C–C–C). They were in good agreement with the characteristic bands found in pure Nile red spectra.[34] These results were consistent with those encapsulating Nile in lysozyme microspheres.[35] The observation of these bands demonstrated that Nile red was incorporated into the gelatin fibers during the electrospinning process.

Fig. 5 shows the TGA curves for gelatin powder, gelatin fibers, and gelatin/Nile red. Gelatin stored in light-proof containers at room temperature remains unchanged for many years. When heated to around 100 °C in the presence of air, gelatin swells, becomes soft and disintegrates into a carbonaceous mass,

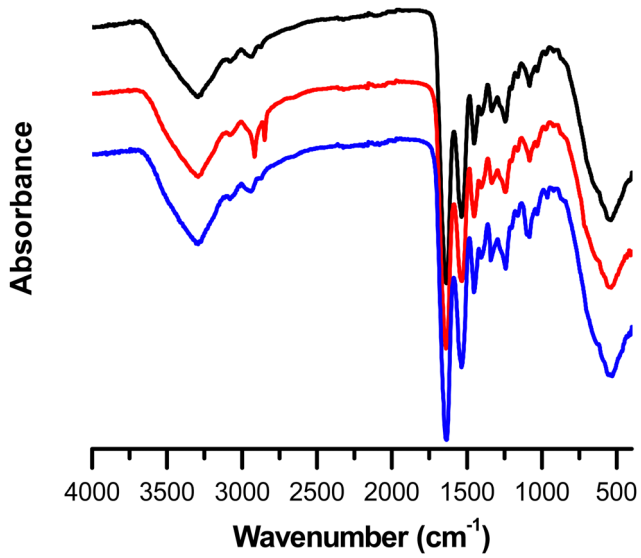

Fig. 4 FTIR spectra of gelatin fibers (▬), gelatin/Nile red (▬) fibers and gelatin/ciprofloxacin (▬) fibers.

releasing pyridine bases and ammonia.[36] This corresponded with the loss of mass shown in Fig. 5. Gelatin is a denatured, partially cleaved collagen with very broad molecular weight distributions, which often still contains cross-linked components resulting from the manufacturing process. The gelatin powder began to lose weight at 260 °C and had lost about 80% of its weight above 700 °C. All gelatin fibers started to lose weight significantly at 244 °C and had lost about 80% and 85% weight above 700 °C for gelatin fiber and gelatin/Nile red, respectively.

Gelatin has three structure types: random coil, single α-helix, and triple helix.[37] The DSC results showed a melting peak at 104.2 °C (Fig. 6), indicating the triple helix structure of commercial gelatin.[28,38] This melting peak no longer appeared for electrospun fibers (Fig. 6). This result may indicate a change in structure consistent with the fact that electrospinning is more successful with a solution in which the gelatin adopts a preferential random coil or α-helix structure induced by the use of TFE. The endothermic peaks at denaturation temperature (T_d) and the corresponding enthalpy reflect the triple helix content. The values of T_d and ΔH_d, obtained from raw gelatin powders and electrospun gelatin nanofibrous membranes, are shown in Table 1. Compared to crude gelatin, the T_d values of electrospun gelatin fibers were higher and the ΔH_d values were lower. This shows that T_d becomes increasingly important as the number of hydrogen bonds is reduced. The decreasing entropy correlates with the increasing mobility of the collagen molecules.[36] However, Fig. S1 and Table S1 (ESI†) demonstrated a temperature shift, with the heating rate showing a time dependency for the loss of structure (denaturation) of the crude gelatin. This could be explained by the phenomenon of apparent melting or the loss of crystalline structure caused by a chemical transformation. As chemical reactions are kinetic processes, the loss of crystallinity during apparent melting is always time-dependent and so occurs at higher temperatures with higher heating rates, and at lower temperatures at slower rates. The denaturation of proteins is one of these chemical transformations leading to a loss of crystalline structure. Modulated DSC makes it possible to monitor and to potentially better understand the thermodynamic and kinetic thermal events in the material. Fig. S2 (ESI†) shows the total heat flow, reversing heat flow and non-reversing heat flow curves. The T_d and ΔH_d values obtained from the raw gelatin powders are shown in Table S2 (ESI†). The total heat flow thermogram showed similarity with the thermograms recorded for the nanofibers, particularly the T_d values. The modulated DSC clearly showed the complexity of gelatin denaturation. We could see that the denaturation phenomenon was both thermodynamic and kinetic, but above all the sum of the two. There was an exothermic phenomenon on the reversing heat flow at 142.8 °C and an endothermic phenomenon on the non-reversing heat flow at 143.0 °C. The sum of these complex phenomena constituted the denaturation observed in Fig. S2 (ESI†). Nevertheless, despite the profile of the total heat flow curve which, due to the presence of T_m, indicated the presence of a triple helix structure, it could not be assumed that nanofibers that did not show a melting peak also had a triple helix structure and may therefore have undergone renaturation after electrospinning.

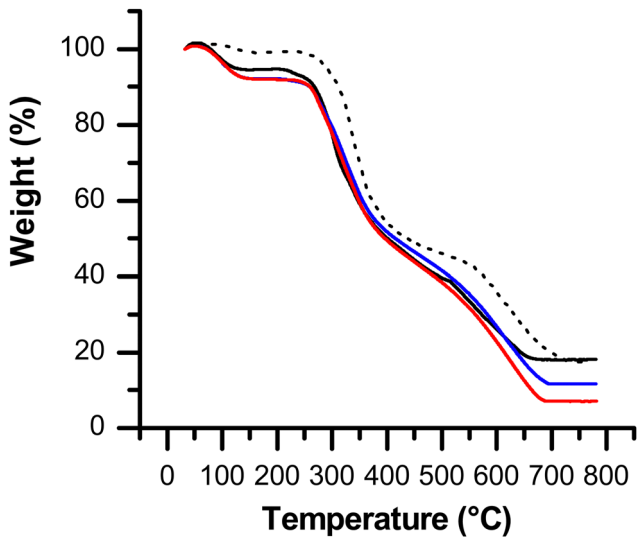

Fig. 5 TGA curves of gelatin powder (···), gelatin fibers (▬), gelatin/Nile red fibers (▬) and gelatin/ciprofloxacin fibers (▬).

Fig. S3 and Table S3 (ESI†) show three different gelatin-based materials: gelatin powder, gelatin nanofibers, and gelatin film. Film and electrospun gelatin had the same thermal profile. This showed that the change in structure was due to the solubilization of the gelatin in TFE. We hypothesized that after solubilization the gelatin structure changed from a majority of triplehelices to single α-helices.

The stress–strain curves of the electrospun gelatin nanofibers are shown in Fig. 7. Based on these curves, the typical mechanical characteristics of Young's modulus stress, and elongation at break are summarized in Table 2. We obtained quasi-similar values to those observed by Zhang *et al.*,[28] with specimen thicknesses of the order of 30 μm. The tensile results

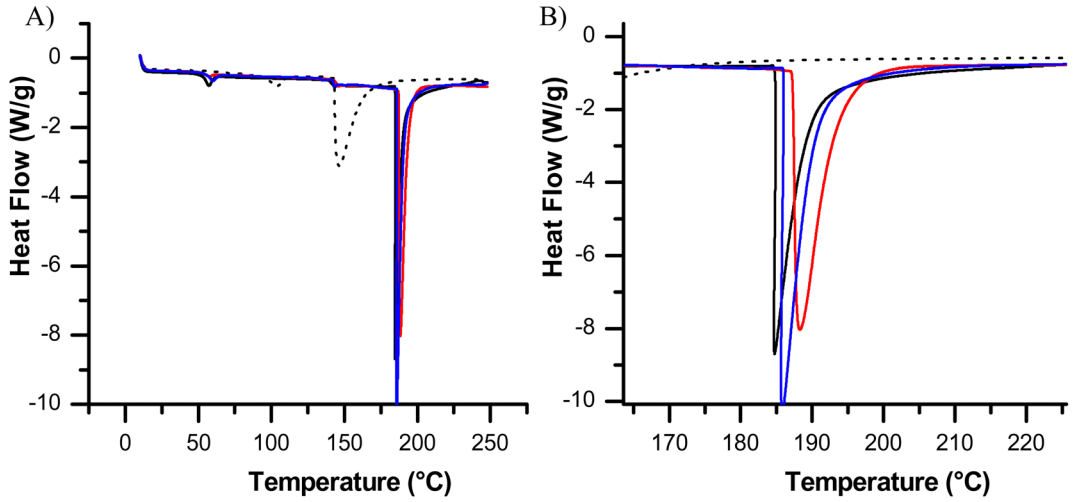

Fig. 6 (A) DSC curves of gelatin powder (···), gelatin fibers (▬), gelatin/Nile red fibers (▬), gelatin/ciprofloxacin fibers (▬), (B) zoom-in of graph A.

Table 1 Characteristic temperatures extracted from DSC analyses

	T_g (°C)	T_d (°C)	ΔH_d (J g^{-1})
Gelatin powder	79.5	146.4	235.6
Gelatin fibers	51.5	184.7	206.8
Gelatin/Nile red fibers	54.1	185.8	196.7
Gelatin/ciprofloxacin fibers	52.2	188.3	194.1

Table 2 Typical mechanical features of fibers

	Gelatin fiber	Gelatin fiber/ Nile red	Gelatin fiber/ ciprofloxacin
Young's modulus (MPa)	40.9 ± 6.3	115.0 ± 13.8	74.40 ± 12.40
Stress (MPa) at break	0.9 ± 0.2	3.5 ± 0.6	2.10 ± 0.60
Elongation at break (%)	2.7 ± 0.2	5.3 ± 1.1	12.00 ± 0.04

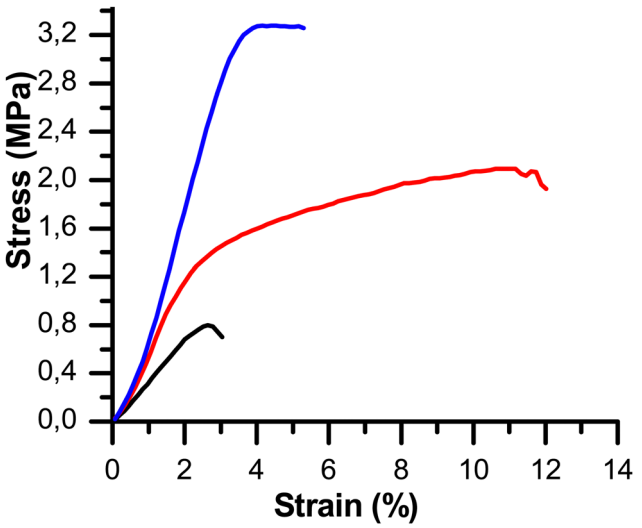

Fig. 7 Stress–strain curves for gelatin nanofibers: gelatin fibers (▬), gelatin/Nile red fibers (▬) and gelatin/ciprofloxacin fibers (▬).

indicated that the gelatin-Nile red mixture improved the mechanical performance of gelatin nanofibers in terms of elasticity and stiffness. We assume that a physical interaction was created between the nanofibers and their additives. We therefore propose that they could act as interfibrillar binders, enabling thicker fibers to be formed from thinner ones, thereby making them more resistant to tensile stress. Studies on collagen, and in particular its mechanical properties, have shown that its properties depend on the arrangement of the fibers and their structure. During tensile testing the collagen molecules slide against each other, causing the fibers to stretch.[36] The presence of Nile red would act as a physical stabilizer of the fibrous protein network and therefore act as a cross-link.

Nile red release from Nile red/gelatin fiber. At 37 °C and pH 7.4, the total release of the Nile red from the fibers occurred within 20 minutes (Fig. S4, ESI†). The behavior of cargo release from this type of material is determined by diffusion, polymer erosion, or a combination of the two. It is noteworthy that at room temperature, after 20 minutes, the gelatin fiber in aqueous solution remains intact. The resultant fiber therefore meets the desired criteria of enabling a rapid release of the cargo. This is an important trait as the fiber is intended for use against antibiotic-resistant bacteria in the wound care field. The aim is for resistant bacteria to be rapidly eliminated so that the wound can be treated.

3.3. Ciprofloxacin loaded inside gelatin fibers

Based on the results obtained from the model drug (Nile red) loading, ciprofloxacin loaded gelatin electrospun mats (ESMs) were fabricated in order to analyze their antibacterial activity against spectinomycin-resistant *E. coli*. SEM analyses showed that the morphology and nanometric size of the fibers were preserved after ciprofloxacin addition (see Fig. 2C). The presence of atomic fluor was detected by energy dispersive X-ray (EDX) analysis, demonstrating the incorporation of ciprofloxacin into the gelatin fibers. In Fig. 4, the FTIR spectrum of ciprofloxacin-loaded gelatin fiber present the following bands:

at 3280 cm^{-1} related to –OH stretching vibration, at 3000 cm^{-1} assigned to alkenes and aromatic C–H stretching (stretching vibration of aromatic enes), at 1643 cm^{-1} indicated carbonyl C=O stretching assigned to quinolones, at 1440 cm^{-1} represented –OH stretching vibration (stretching vibration of carboxylic acid), and at 1340 cm^{-1} suggested bending vibration of C–F. These bands were in good agreement with the characteristic bands found in pure ciprofloxacin spectra. The observation of these bands evidenced that ciprofloxacin was incorporated into the gelatin fibers. TGA analysis of the fiber showed that it started to lose weight at 244 °C and had lost about 90% of its weight above 700 °C. DSC measurements were also performed, and the same behaviour as gelatin/Nile red fibers was observed (Fig. 6), *i.e.* close T_d values were obtained for antibiotic gelatin fibers (188.3 °C) than for gelatin-only fibers (184.7 °C) and Nile red-loaded gelatin fibers (185.8 °C). The tensile results indicated that the incorporation of ciprofloxacin improved the mechanical performance of gelatin nanofibers in terms of elasticity and stiffness (Fig. 7 and Table 1). Indeed, for ciprofloxacin- loaded gelatin fiber, Young's modulus, the stress at break, and the elongation at break are 74.40 ± 12.40 MPa, 2.10 ± 0.60 MPa and 12.00 ± 0.04%, respectively. In contrast to unloaded gelatin fibers, the Young's modulus, the stress at break, and the elongation at break are 40.9 ± 6.3 MPa, 0.9 ± 0.2 MPa and 2.7 ± 0.2%, respectively.

Bactericidal activity of gelatin electrospun mats loaded with ciprofloxacin antibiotic. Designing an ESM with both biocompatibility and antibiotic activity against antibiotic-resistant bacteria could have useful applications for wound dressings. The antimicrobial activity of gelatin loaded with ciprofloxacin was characterized by agar diffusion tests. The first consisted of a direct biofilm contact test, which aimed to assess the efficacy of the material for the clearance of antibiotic-resistant bacteria on infected wound sites. We also performed an inhibitory growth test in order to assess the ability to prevent the bacterial contamination of the treated areas. In both tests, clear zones indicating the inhibition of spectinomycin-resistant bacteria growth appeared around the ciprofloxacin-loaded gelatin fiber material. Their mean areas were recorded over 24 and 48 hours. It is noteworthy that the gelatin fibers had no impact on the bacteria activity (Fig. 8).

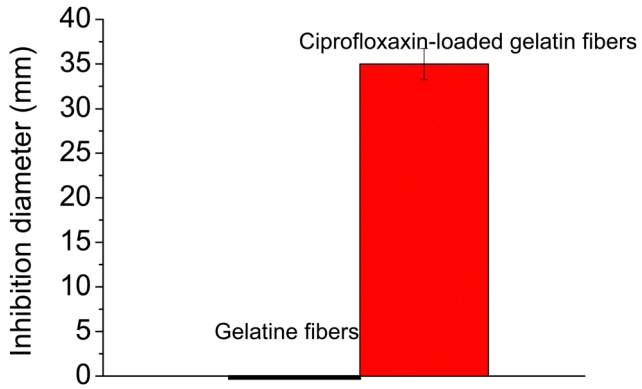

Fig. 8 Diameters of inhibition zones against spectinomycin-resistant *E. coli* when using gelatin fibers and ciprofloxacin-loaded gelatin fibers.

Nutrient agar plates that were not inoculated or that contained a deposited gelatin fiber had clear agar. Nutrient agar plates that were seeded with antibiotic-resistant bacteria exhibited uniform biofilms on their surfaces that gave a uniform turbidity to the plates. Ciprofloxacin is a second-generation fluoroquinolone that is active against many Gram-negative and Gram-positive bacteria. It acts by inhibiting bacterial DNA gyrase and topoisomerase IV.[39] Ciprofloxacin binds to bacterial DNA gyrase and prevents it from supercoiling the bacterial DNA, thereby preventing bacterial replication.[40]

The gelatin fibers loaded with ciprofloxacin allowed for the removal and the prevention of growth of spectinomycin-resistant *E. coli*. Moreover, the antibacterial action of the antibiotic-loaded material was rapid: a significant effect was visible within 20 minutes (*i.e.* the release rate of the antibiotic (ciprofloxacin) occurred within 20 minutes at 37 °C and pH 7.4, as for the Nile red from the fibers), which was in concordance with our results assessing *in vitro* Nile red release. The effect persisted for at least 72 hours. The antibacterial activity of the ESM against the bacteria indicated that the integrity of ciprofloxacin was not affected by the high voltage used during electrospinning. The bacterial contamination (bacteria resistant to antibiotics) of a wound may lead to an infection. Therefore, the designed ESMs may be a suitable material for the treatment of infected wound sites or wound infection prophylaxis.

We then examined if the bacteria were viable or not at the end of the bacterial assay. For this, bacteria were stained with acridine orange for discriminating between living and dead bacteria.[41] Indeed, acridine orange is a cell-permeant nucleic acid binding probe and thus allows one to differentiate between double-stranded and single-stranded nucleic acids. Acridine orange emits red fluorescence when bound to denatured single stranded DNA found in dead bacteria and emits green fluorescence when bound to double stranded DNA as found in living bacteria. Red fluorescence was seen after staining bacteria (Fig. 9B), evidencing the death of bacterial cells due to exposure to the ciprofloxacin-gelatin fiber. In contrast, green fluorescence was shown for bacteria exposed to the gelatin fiber (Fig. 9A), evidencing that the bacteria are alive when no antibiotic is loaded inside the fiber. It is important to note that similar results were obtained with a strain that is not resistant to antibiotics, *i.e. E. Coli*.

4. Conclusion

Gelatin ESMs were fabricated for antibiotic delivery purposes. Electron microscopy showed that smooth gelatin-based fibers were produced and that their structure remained intact after hydrophobic cargo loading. The mechanism of hydrophobic cargo release from the ESM fiber was first examined using Nile red dye. DSC measurements indicated that the gelatin-based fibers may have undergone renaturation after electrospinning. Using DMA measurement, we found that the presence of hydrophobic cargo enhanced the mechanical properties of the gelatin fiber. This result is of interest as previous literature has shown that enhanced mechanical properties in gelatin fibers

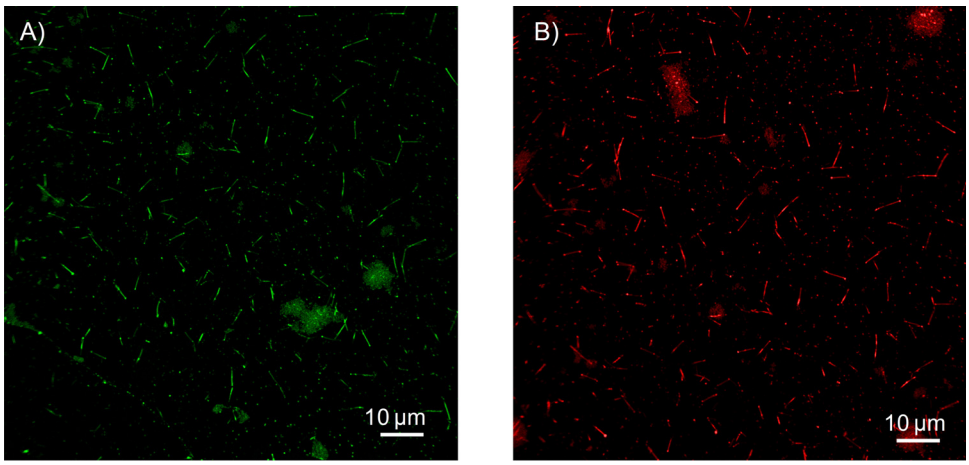

Fig. 9 Spectinomycin-resistant *E. coli* stained with acridine orange after the antibacterial assay, (A) in contact with gelatin fiber and (B) in contact with the ciprofloxacin-gelatin fiber.

occur following film crosslinking. We then loaded ciprofloxacin inside the fiber as a hydrophobic cargo and showed that the ESMs are highly active against spectinomycin-resistant *E. coli*.

This studied antibiotic-loaded gelatin ESM is a promising material for wound dressings due to its antibiotic properties. In the future, we plan to test the effect of the designed fiber on other antibiotic-resistant *E. Coli* strains, as well as other species of bacteria.

Conflicts of interest

There are no conflicts to declare.

References

1 J. Acar and G. Moulin, *Rev. Sci. Tech.*, 2012, **31**, 23–31.
2 D. van Duin and D. L. Paterson, *Infect. Dis. Clin.*, 2020, **34**, 709–722.
3 J. O'neill, *Rev. Antimicrob. Resist.*, 2014, **https://wellcomecollection.org/works/rdpck35v**.
4 A. Delamou, B. S. Camara, S. Sidibé, A. Camara, N. Dioubaté, A. M. El Ayadi, K. Tayler-Smith, A. H. Beavogui, M. D. Baldé and R. Zachariah, *J. Public Health Africa*, 2019, **10**(1), 818.
5 E. J. Woodmansey and C. D. Roberts, *Int. Wound J.*, 2018, **15**, 1025–1032.
6 H. Janssen, I. Janssen, P. Cooper, C. Kainyah, T. Pellio, M. Quintel, M. Monnheimer, U. Groß and M. H. Schulze, *Emerging Infect. Dis.*, 2018, **24**, 916.
7 M. Mama, A. Abdissa and T. Sewunet, *Ann. Clin. Microbiol. Antimicrob.*, 2014, **13**, 1–10.
8 K. I. Wolska, K. Grzes and A. Kurek, *Pol. J. Microbiol.*, 2012, **61**, 95–104.
9 T. Sukumar, D. Nallasamy, K. Kadirvelu and H. Kim, *Mater. Sci. Eng., B*, 2017, **217**, 36–48.
10 J. Ramier, D. Grande, T. Bouderlique, O. Stoilova, N. Manolova, I. Rashkov, V. Langlois, P. Albanese and E. Renard, *J. Mater. Sci.: Mater. Med.*, 2014, **25**, 1563–1575.
11 L. J. Villarreal-Gómez, J. M. Cornejo-Bravo, R. Vera-Graziano and D. Grande, *J. Biomater. Sci., Polym. Ed.*, 2016, **27**, 157–176.
12 X. Liu, T. Lin, J. Fang, G. Yao, H. Zhao, M. Dodson and X. Wang, *J. Biomed. Mater. Res., Part A*, 2010, **94**, 499–508.
13 J. Xue, M. He, H. Liu, Y. Niu, A. Crawford, P. D. Coates, D. Chen, R. Shi and L. Zhang, *Biomaterials*, 2014, **35**, 9395–9405.
14 M. Zamani, M. P. Prabhakaran and S. Ramakrishna, *Int. J. Nanomed.*, 2013, **8**, 2997–3017.
15 S. Young, M. Wong, Y. Tabata and A. G. Mikos, *J. Controlled Release*, 2005, **109**, 256–274.
16 M. Li, M. J. Mondrinos, M. R. Gandhi, F. K. Ko, A. S. Weiss and P. I. Lelkes, *Biomaterials*, 2005, **26**, 5999–6008.
17 M. Li, Y. Guo, Y. Wei, A. G. MacDiarmid and P. I. Lelkes, *Biomaterials*, 2006, **27**, 2705–2715.
18 Z.-M. Huang, Y. Z. Zhang, S. Ramakrishna and C. T. Lim, *Polymer*, 2004, **45**, 5361–5368.
19 C. S. Ki, D. H. Baek, K. D. Gang, K. H. Lee, I. C. Um and Y. H. Park, *Polymer*, 2005, **46**, 5094–5102.
20 T. Thairin and P. Wutticharoenmongkol, *J. Ind. Text.*, 2022, **51**, 1296S–1322S.
21 A. R. Unnithan, N. A. Barakat, P. B. Pichiah, G. Gnanasekaran, R. Nirmala, Y. S. Cha, C. H. Jung, M. El-Newehy and H. Y. Kim, *Carbohydr. Polym.*, 2012, **90**, 1786–1793.
22 A. Toncheva, D. Paneva, V. Maximova, N. Manolova and I. Rashkov, *Eur. J. Pharm. Sci.*, 2012, **47**, 642–651.
23 S. P. Parwe, P. N. Chaudhari, K. K. Mohite, B. S. Selukar, S. S. Nande and B. Garnaik, *Int. J. Nanomed.*, 2014, **9**(1), 1463–1477.
24 K. Kataria, A. Gupta, G. Rath, R. B. Mathur and S. R. Dhakate, *Int. J. Pharm.*, 2014, **469**, 102–110.
25 H. Nageh, M. Ezzat, M. Ghanim and A. Hassanin, *UK J. Pharm. Biosci.*, 2014, **2**(3), 01–05.
26 A. Kyzioł, J. Michna, I. Moreno, E. Gamez and S. Irusta, *Eur. Polym. J.*, 2017, **96**, 350–360.
27 W. Lu, H. Xu, B. Zhang, M. Ma and Y. Guo, *J. Nanosci. Nanotechnol.*, 2016, **16**, 2360–2364.

28 Y. Z. Zhang, J. Venugopal, Z. M. Huang, C. T. Lim and S. Ramakrishna, *Polymer*, 2006, **47**, 2911–2917.
29 L. Boulos, M. Prevost, B. Barbeau, J. Coallier and R. Desjardins, *J. Microbiol. Methods*, 1999, **37**, 77–86.
30 M. Nagura, H. Yokota, M. Ikeura, Y. Gotoh and Y. Ohkoshi, *Polym. J.*, 2002, **34**, 761–766.
31 J. A. Matthews, G. E. Wnek, D. G. Simpson and G. L. Bowlin, *Biomacromolecules*, 2002, **3**, 232–238.
32 D. M. Hashim, Y. B. C. Man, R. Norakasha, M. Shuhaimi, Y. Salmah and Z. A. Syahariza, *Food Chem.*, 2010, **118**, 856–860.
33 M. C. Chang, C. C. Ko and W. H. Douglas, *Biomaterials*, 2003, **24**, 2853–2862.
34 D. Kępińska, A. Budniak, K. Kijewska, G. J. Blanchard and M. Mazur, *Polymer*, 2013, **54**, 4538–4544.
35 B. Bhargawa, V. Sharma, M.-R. Ganesh, F. Cavalieri, M. Ashokkumar, B. Neppolian and A. Sundaramurthy, *Ultrason. Sonochem.*, 2022, **86**, 106016.
36 M. Meyer, *BioMed. Eng. OnLine*, 2019, **18**, 24.
37 P. Sajkiewicz and D. Kołbuk, *J. Biomater. Sci., Polym. Ed.*, 2014, **25**, 2009–2022.
38 A. Duconseille, F. Wien, F. Audonnet, A. Traore, M. Refregiers, T. Astruc and V. Santé-Lhoutellier, *Food Hydrocolloids*, 2017, **66**, 378–388.
39 F. Pietsch, J. M. Bergman, G. Brandis, L. L. Marcusson, A. Zorzet, D. L. Huseby and D. Hughes, *J. Antimicrob. Chemother.*, 2017, **72**, 75–84.
40 M. LeBel, *Pharmacotherapy*, 1988, **8**, 3–33.
41 D. E. Francisco, R. A. Mah and A. C. Rabin, *Trans. Am. Microsc. Soc.*, 1973, 416–421.